Beam Shaping by Mode Superposition With Coefficient Optimization

Guowen Zhang, Hang Sun, Ziyang Chen, *Senior Member, IEEE*, Yanli Zhang, Jixiong Pu, and Jianqiang Zhu

***Abstract*—Beam shaping is of significance for applications in various fields, including laser fusion, laser processing, and optical manipulation. One conventional approach for beam shaping is using the superposition of eigenmodes, such as the Hermite-Gaussian (HG) modes. However, despite the generation of a flat-top beam by HG modes with identical coefficients, it is challenging to achieve other specific intensity distributions by this method. In this study, we validate the feasibility of the beam patterns modulation by optimizing the coefficients of the superimposed modes using an optimization algorithm. Beyond producing square flat-top spots with controllable size and intensity, this method can also achieve specialized intensity distributions including hollow square spots.**

***Index Terms*—Flat-top beam, beam shaping, mode superposition, optimization algorithm.**

I. Introduction

GENERATION of beams with specific intensity distribution is a fundamental prerequisite for applications ranging from the interaction between laser and matter [1], [2] to particle manipulation [3], [4] and laser fusion [5], [6]. Chen et al. demonstrated that, with suitable ratio of particle diameter to wavelength, the flat-top focus exhibits the largest trapping efficiency in comparison with a Gaussian beam and a donut shaped beam [3]. In laser processing, a flat-top beam with a uniform intensity distribution is usually required for implementation of uniform processing [5]. In inertial confinement fusion, the employment of beams with smooth intensity distributions proves to be an effective strategy for mitigating laser plasma instability [7]. Studies have shown that using a flat-top beam can improve the impact of pointing errors on small satellite optical communication [8]. Owing to the important potential applications of flat-top beams, their generation has attracted considerable attention [9], [10], [11]. Researchers have proposed several methods to produce flat-top beams, such as employing annular cavity structures [12], making aspheric lenses with 3D printing technology [13], implementing beam shaping inside the cavity [14], and utilizing axicons [15] or special diffraction optical elements [16]. Zhu et al. utilized fiber-coupled semiconductor lasers as the light source and a beam homogenization system to achieve a flat-top beam output with a power of 1940 W [17].

In addition, the superposition of multiple beams to produce flat-top beams is also a common method [18], [19]. By superimposing multiple HG mode beams, different types of intensity distributions can be produced [20], [21]. For example, employing identical coefficient for each superimposed mode yields a flat-top beam with a uniform intensity distribution. Nevertheless, in laser processing and other applications, it is necessary to effectively control the spot size of the flat-top beam and generate some specific intensity distributions according to different processing requirements [22], [23]. However, the conventional method of using the same coefficient cannot flexibly control the properties of the superimposed spot.

The optimized algorithm has been introduced in shaping the optical field [16], [24]. One notable example is Gerchberg-Saxton (GS) algorithm [25], which is a key optimization model for calculation of diffractive optical elements [26], [27] and computer generated holograms [28]. Wang et al introduced gradient descent and weighting strategy to address the stagnation problem of GS algorithm. [29]. In analogy with optical image encryption, Wu et al. performed the algorithm to calculate the optimized patterns, by which the mode conversation between beams and beam distortion compensation can be achieved [30]. With the algorithm-assisted design, these optical elements can greatly improve the capability of beam shaping. Even in rather complicated and random scattering process, the optimization algorithm can still be utilized to realize the light focusing, spectrum filtering etc [31], [32], [33], [34].

Beam shaping can also be realized by the superposition of fundamental modes, wherein the resulting intensity distribution depends on the coefficients and quantity of the involved modes. Calculating the coefficients of fundamental modes to generate a beam pattern with a specific distribution becomes intricate, particularly when dealing with a large number of involved modes. To tackle this complexity, we propose a method to calculate the coefficients of the HG beams by introducing an optimization algorithm. By setting the expected target light field and employing it as the optimization target of the algorithm,

Manuscript received 24 April 2024; revised 20 May 2024; accepted 21 May 2024. Date of publication 28 May 2024; date of current version 24 June 2024. This work was supported in part by the Strategic Priority Research Program of Chinese Academy of Sciences under Grant XDA 25020203 and in part by the National Natural Science Foundation of China (NSFC) under Grant 62375092. *(Corresponding author: Jianqiang Zhu.)*

Guowen Zhang is with the National Laboratory on High Power Laser and Physics, Shanghai Institute of Optics and Fine Mechanics, Chinese Academy of Sciences, Shanghai 201800, China, and also with the University of Chinese Academy of Science, Beijing 100049, China (e-mail: guowenzhang@siom.ac.cn).

Hang Sun and Ziyang Chen are with the Fujian Key Laboratory of Light Propagation and Transformation, College of Information Science and Engineering, Huaqiao University, Xiamen 361021, China (e-mail: 1301753647@qq.com; ziyang@hqu.edu.cn).

Yanli Zhang, Jixiong Pu, and Jianqiang Zhu are with the National Laboratory on High Power Laser and Physics, Shanghai Institute of Optics and Fine Mechanics, Chinese Academy of Sciences, Shanghai 201800, China (e-mail: zhangyl@siom.ac.cn; jxpu@163.com; jqzhu@mail.shcnc.ac.cn).

Digital Object Identifier 10.1109/JPHOT.2024.3405943

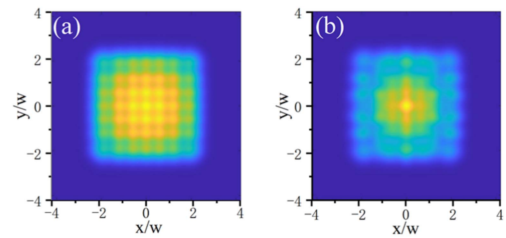

Fig. 1. The influence of the coefficient of HG modes on the superposition intensity. (a) Same coefficient. (b) Random coefficient.

the algorithm continuously iterates to calculate improved coefficients, and finally obtains suitable coefficients to achieve the expected target intensity distribution. This approach is not only capable of producing conventional flat-top beams but also enables the realization of more intricate spot shapes.

II. Theoretical Analysis

Hermite-Gaussian modes are orthogonal solutions to the paraxial wave equation, which can be directly generated from a laser cavity [35]. Various methods, including V-type cavity [36] and end-pumped solid-state lasers with an opaque-wire-inserted laser resonator [37] or with "off-axis pumping" scheme [38], have been developed to generate high order HG modes.

The light field of HG mode can be expressed as [20], [39]:

$$\psi_{mn}\ (x, y) = \sqrt{\frac{2}{2^{m+n}\pi w^2 m!n!}}\, H_m\left(\frac{\sqrt{2}x}{w}\right) H_n\left(\frac{\sqrt{2}y}{w}\right) \times \exp\left(-\frac{x^2+y^2}{w^2}\right), \tag{1}$$

where $H_m(x)$ denotes the Hermit polynomial of order m, w represents the beam size.

The superposition of multiple HG modes can be represented as

$$I\ (x, y) = \sum_{m=0}^{m1}\sum_{n=0}^{n1} \lambda_{mn} \left|\psi_{mn}\,(x, y)\right|^2, \tag{2}$$

where λ_{mn} represents the coefficient of the mn-th mode, with m_1 and n_1 are the number of modes involved in the superposition. This equation indicates that the intensity of the superimposed light is related to the coefficient of each mode involved in the superposition. To generate a flat-top beam, the coefficients of the modes are usually set to be the same. Taking the superposition of 49 modes (from HG_{00} to HG_{66}) as an example, Fig. 1 illustrates the impact of the coefficients of each mode on the intensity of the superimposed light. With the same coefficient of each mode, a flat-top beam with a uniform intensity distribution is obtained. On the other hand, when the coefficients of modes are random, the intensity strongly fluctuates. These results imply that the intensity distribution of the superimposed light can be effectively controlled by adjusting the coefficients of the modes. Therefore, a light spot with a predetermined distribution can be obtained using the appropriate coefficients.

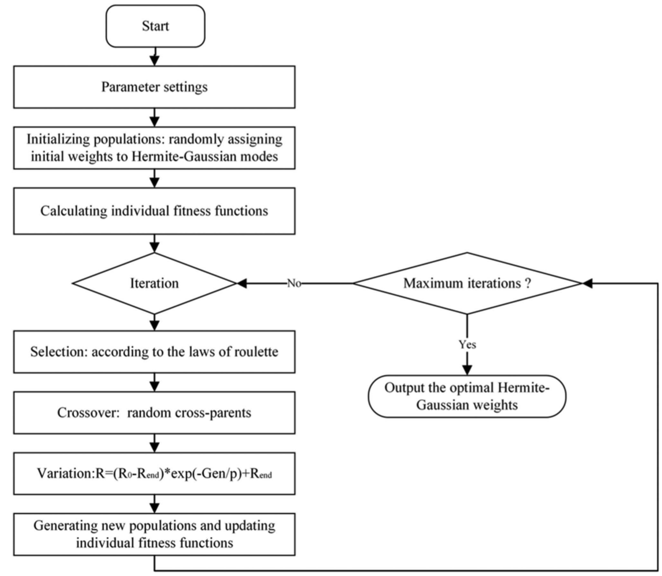

Fig. 2. Flow chart of algorithm.

Genetic algorithm is a classic optimization algorithm that employs the principles of biological evolution to find the optimal solution. The strong anti-noise ability renders it can be widely used in various types of optimization calculations [40]. The genetic algorithm is chosen as the optimization algorithm to find the appropriate mode coefficient. Specifically, we regard the mode coefficient of input HG modes as an individual in the population, and search for the optimal mode coefficient through the following steps. Firstly, a random initial population is generated, and the fitness function value corresponding to each individual is calculated. We choose the Pearson correlation coefficient (PCC) as the fitness function, which effectively measures the difference between the beam pattern after superimposing multiple modes and the expected beam pattern. The higher the PCC value, the better the superimposing effect. Then, we conduct parent selection according to the roulette wheel selection rule, that is, the higher the fitness function value, the greater the chance of being selected as parents. To generate new offspring individuals, we perform crossover operation according to the following formula

$$Child\ =\ ma \times T + pa \times (1 - T), \tag{3}$$

where ma and pa denote two parent coefficients, and T is a random binary breeding template array.

After that, we perform mutation operation on the newly generated individuals, further enriching the gene pool of the population. Subsequently, fitness function values are calculated for the generated new individuals, and they are sorted together with the parent population, retaining individuals with higher fitness to form a new population. Iterating in this way will eventually yield the ideal mode coefficient. Throughout the entire search process, we take the number of HG modes as the dimension, assigning a coefficient to each HG mode to achieve coefficient regulation for different target modes. The flowchart of the genetic algorithm is shown in Fig. 2.

The parameters of the algorithm are chosen as follows: the maximal iteration number is $Gen = 1000$, the size of initial population is $Np = 50$, the offspring number is $G = 25$, the initial and the final mutation factor are $R_0 = 0.1$ and $R_{end} = 0.0025$ respectively, the mutation rate of the offspring can be calculated by the formula $R = (R_0 - R_{end}) \times e^{-\frac{Gen}{p}} + R_{end}$, where $p = 200$ is the decay factor.

Based on the superposition of HG modes, a light spot with a relatively uniform intensity distribution can be produced if the coefficient of each mode is equal, as shown in Fig. 1(a). We introduce optimization algorithms to regulate the coefficients of the superimposed modes to achieve light spots with different sizes and a uniform intensity distribution. To ensure the iterative algorithm converge to this intensity distribution, the PCC between the target intensity distribution and the iterative intensity distribution is designed as the fitness function, which measures the degree of correlation between the two intensity distributions. The PCC is defined as [41]: (4) shown at the bottom of the this page.

where

$$\langle I_i \rangle = \frac{1}{NN} \sum_{x=1}^{N} \sum_{y=1}^{N} I_i(x, y) \quad (5)$$

$$\langle I_o \rangle = \frac{1}{NN} \sum_{x=1}^{N} \sum_{y=1}^{N} I_o(x, y) \quad (6)$$

with $I_i(x,y)$ represents the intensity value corresponding to the coefficient calculated during the iterative process, and $I_o(x,y)$ represents the preset target intensity distribution, x and y represent the coordinates.

III. Numerical Simulations

Taking the square flat-top beam designed in Fig. 3(a) as the target intensity distribution, we regulate the coefficients of 49 modes (from HG_{00} to HG_{66}) to generate a light spot that resembles the predesigned one. The results in Fig. 3(b) and (c) show that the intensity distribution is in good agreement with the expected intensity distribution. To quantitively evaluates the intensity uniformity, we depict the residue value of the intensity magnitude within the modulation region. The vertical coordinate of residue map is defined as the ratio of subtracted intensity value of a point from the average intensity value of the region over the average intensity value of the region. As illustrated in Fig. 3(e), the maximal residue value within the region is less than 110% of the average value of the region, and residue values for the majority of points fall within the range of ± 10%. Furthermore, compared with the light spot with equal coefficient (Fig. 1(a)), the size of the superimposed square light spot can be effectively controlled. The optimized coefficient of the modes corresponding to the obtained intensity distribution is presented in Fig. 3(f). Although a total of 49 modes were used for optimization, the top 10 modes with the highest coefficient proportions account for over 90%, while the coefficient of the other modes is negligible, indicating that the use of these top 10 modes in superposition can basically achieve a square light spot with good intensity uniformity.

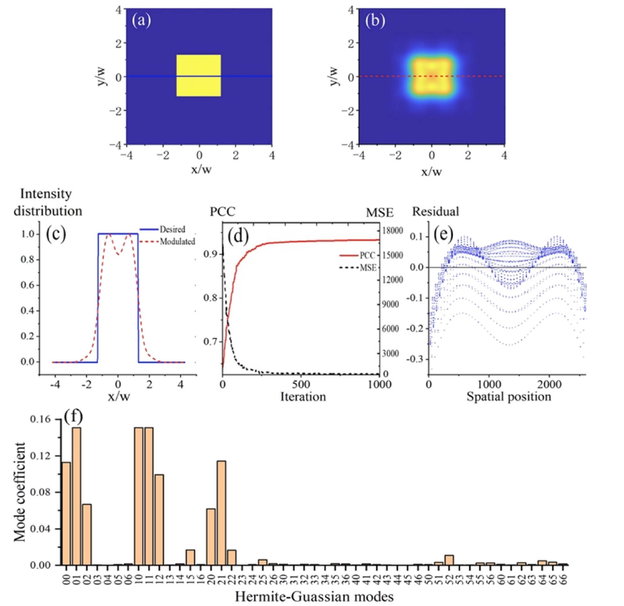

Fig. 3. Generation of a square flat-top beam by the superposition of 49 HG modes. (a) Desired intensity distribution; (b) Intensity distribution after coefficient optimization; (c) The intensity profile along the blue solid line in (a) and red dashed line in (b); (d) The evolution of PCC and MSE during iteration; (e) The residue value of the intensity in the modulation region; (f) The optimized coefficient of the modes.

To evaluate the modulation effect, we introduce PCC to quantitatively measure the similarity between the modulated intensity and the expected intensity, and introduce MSE (Mean Square Error) to quantitatively calculate the fluctuation of the intensity in the target area. The definition of MSE is as follows:

$$MSE = \frac{1}{N^2} \sum_{x=1}^{N} \sum_{y=1}^{N} \left(I(x, y) - \overline{I(x, y)} \right)^2 \quad (7)$$

where $I(x,y)$ represents the intensity in the target area, and $\overline{I(x,y)}$ represents the average intensity in the target area. As the number of iterations increases, PCC increases from the initial 0.64 to 0.939 and tends to stabilize (Fig. 3(d)). And the MSE decreases rapidly in the first 100 iterations, and the decreasing trend slows down after 100 iterations (Fig. 3(d)).

Furthermore, a more complex beam pattern, a square flat-top beam with a central circular dark core (Fig. 4(a)), is designed as the optimization target. It is challenging to achieve such a complex beam pattern through traditional mode superposition methods. Based on the genetic algorithm and according to the

$$\gamma = \frac{\sum_{x=1}^{N} \sum_{y=1}^{N} [I_i(x, y) - \langle I_i \rangle][I_o(x, y) - \langle I_o \rangle]}{\left\{ \sum_{x=1}^{N} \sum_{y=1}^{N} [I_i(x, y) - \langle I_i \rangle]^2 \sum_{x=1}^{N} \sum_{y=1}^{N} [I_o(x, y) - \langle I_o \rangle]^2 \right\}^{\frac{1}{2}}} \quad (4)$$

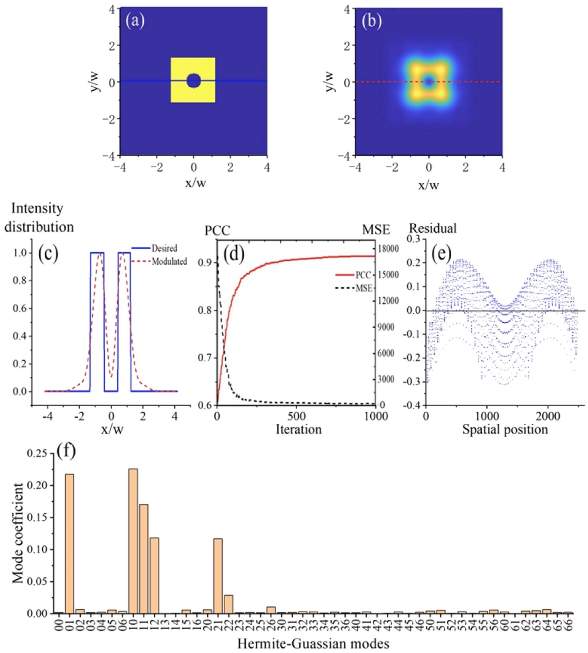

Fig. 4. Generation of a square spot with dark core by the superposition of 49 HG modes. (a) Desired intensity distribution; (b) Intensity distribution after coefficient optimization; (c) The intensity profile along the blue solid line in (a) and red dashed line in (b); (d) The evolution of PCC and MSE during iteration; (e) The residue value of the intensity in the modulation region; (f) The coefficient of the modes.

optimization target, the optimized coefficient of each mode is calculated, and a light spot that that is very close to the target distribution is finally achieved (Fig. 4(b) and (c)). The PCC index between the modulated light spot and the target light spot reached 0.918 (Fig. 4(d)). As the iterations progressed, MSE gradually decreases, indicating that the fluctuation of the intensity is gradually suppressed, and a more uniform intensity distribution is achieved (Fig. 4(d)). The residue values in Fig. 4(e) indicates that the residue intensity value for the majority of the points within the modulated region fall within the range of $\pm$ 20%. The mode coefficients (Fig. 4(f)) show that the top 5 modes with the highest coefficient proportions account for over 80% of the total coefficient, implying that using these 5 modes in superposition can basically achieve a similar intensity distribution.

We further reduce the HG modes to 9, ranging from HG_{00} to HG_{22}, as an alternative mode superposition scheme for beam shaping, as shown in Fig. 5. We consider three desired superimposed patterns, dividing them into two regions, central and surrounding, with an intensity ratio of 1:0.25. Both the size of the central region and surrounding one can be flexibly controlled. For example, Fig. 5(b1) and (c1) exhibit the same modulation area, yet the central region accounts for 39% and 56.2% of the modulated pattern, respectively. This numerical simulation validates the feasibility of generating specialized beam pattern by the superposition of fundamental modes, even with a limited number of modes.

This study is rooted in the concept of calculating coefficients for beams through an optimization algorithm, which may provide a solution for beam shaping. This concept could be useful in scenarios where multiple beams overlap, and the intensity distribution of these beams is known or premeasured. By establishing the desired beam pattern as the objective and executing the optimization algorithm, one can compute the coefficients for these beams. Subsequently, the transmittance of the beams can be experimentally controlled by applying the optimized coefficients along with attenuation. Through this approach, one can finally control the light field in the overlap region.

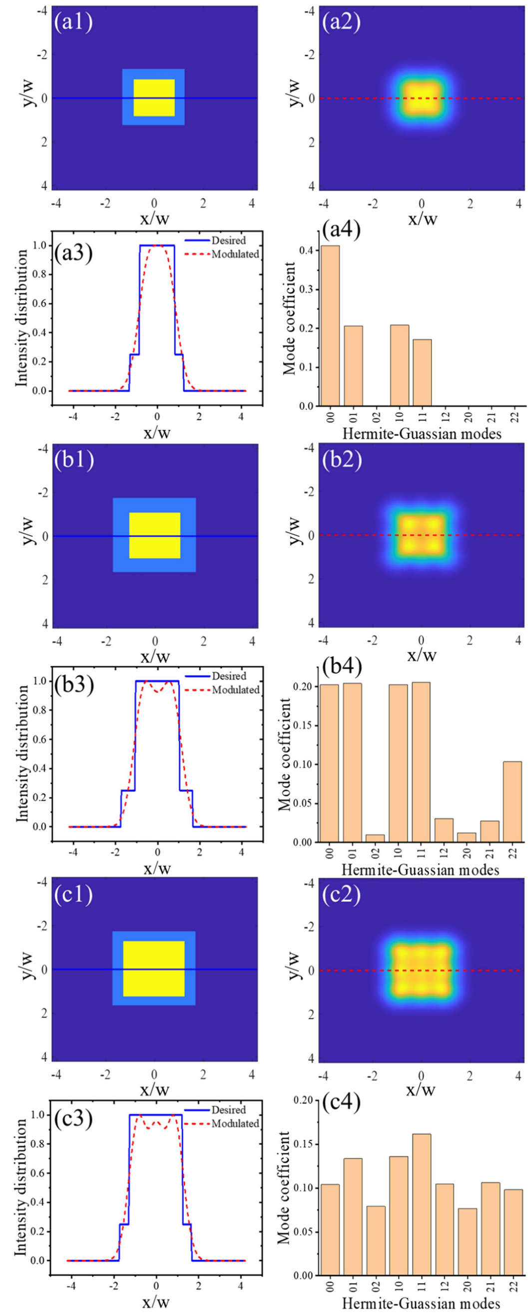

Fig. 5. Generation of a square spot with two different intensity regions by the superposition of 9 HG modes. (a1), (b1), (c1): Desired intensity distribution; (a2), (b2), (c2): Intensity distribution after coefficient optimization; (a3), (b3), (c3): Intensity profile along the blue solid line in (a1), (b1), (c1) and dashed red line in (a2), (b2), (c2); (a4), (b4), (c4): The coefficient of the modes corresponding to the modulated intensity of (a2), (b2), (c2).

IV. Conclusion and Discussions

Based on the principle of mode superposition, we proposed a method to control the intensity distribution of the superimposed light spot by regulating the coefficients of the superimposed modes. The traditional HG mode superposition method usually sets each mode to have the same coefficient, which can generate a square light spot after mode superposition. However, the intensity distribution of this light spot is difficult to be flexibly controlled. We applied genetic algorithm to achieve flexible control of the light spot by regulating the coefficients of the modes. Using a predesigned beam pattern as optimization target of the algorithm and by iteratively calculating the matching coefficient of the modes, a light spot that is consistent with the target intensity distribution can be achieved. Based on this method, not only square flat-top beam, but also more complex square intensity distributions with a circular hollow or different intensity magnitude regions can be achieved, and the light spot has a relatively good intensity uniformity.

References

[1] J. Cheng et al., "A review of ultrafast laser materials micromachining," *Opt. Laser Technol.*, vol. 46, pp. 88–102, 2013.

[2] X. Hao, Z. Zhong, and B. Zhang, "Influence of spatiotemporal coherence of broadband laser on beam smoothing of ISI," *Opt. Commun.*, vol. 520, 2022, Art. no. 128256.

[3] H. Chen and K. C. Toussaint, "Application of flat-top focus to 2D trapping of large particles," *Opt. Exp.*, vol. 22, pp. 6653–6660, 2014.

[4] K. Krishna, J. A. Burrow, M. Diouf, J. Sun, M. Harling, and K. C. Toussaint Jr., "Using flat-top light sheet generated by femtosecond-pulsed laser for optical manipulation of microscopic particles," *Proc. SPIE*, vol. 12649, pp. 134–142, 2023.

[5] W. Yuan, H. Chen, S. Li, Y. Heng, S. Yin, and Q. Wei, "Understanding of adopting flat-top laser in laser powder bed fusion processed Inconel 718 alloy: Simulation of single-track scanning and experiment," *J. Mater. Res. Technol.*, vol. 16, pp. 1388–1401, 2022.

[6] Y. Wang and J. Shi, "Developing very strong texture in a nickel-based superalloy by selective laser melting with an ultra-high power and flat-top laser beam," *Mater. Characterization*, vol. 165, 2020, Art. no. 110372.

[7] P. A. Norreys, N. B. Farhat, Y. Sentoku, L. O. Silva, R. A. Smith, and R. M. G. M. Trines, "Intense laser-plasma interactions: New frontiers in high energy density physics," *Phys. Plasmas*, vol. 16, no. 4, 2009, Art. no. 041002.

[8] Z. Hu, D. Jiang, X. Liu, B. Zhu, Q. Zeng, and K. Qin, "Performance research on flat-topped beam-based small satellites free space optical communication," *Opt. Commun.*, vol. 487, 2021, Art. no. 126802.

[9] Y. Deng, X. Ji, H. Yu, X. Li, H. Wang, and L. Chen, "Uniform irradiation generated by beam self-focusing in the inhomogeneous atmosphere," *Opt. Exp.*, vol. 27, no. 10, pp. 14585–14593, 2019.

[10] D. Y. Alsaka, C. Arpali, S. A. Arpali, and M. F. Altemimi, "Dynamic flat-topped laser beam shaping method using mixed region amplitude freedom algorithm," *Appl. Phys. B*, vol. 128, no. 8, 2022, Art. no. 137.

[11] R. S. Chang, C. S. Chen, C. L. Lee, Y. J. Cui, W. J. Chung, and I. C. Hsu, "Heuristic self-photography approach for flat-top beam generation with arbitrary beam intensity distribution," *Optik*, vol. 218, 2020, Art. no. 164964.

[12] A. Lopez-Vazquez, Y. M. Torres, M. S. Billion, W. M. Pimenta, J. A. Franco-Vollafane, and E. Gomez, "Experimental generation of a flat-top beam profile in a stable ring cavity," *Opt. Lett.*, vol. 44, no. 17, pp. 4428–4431, 2019.

[13] B. D. Price, S. N. Lowry, I. D. Hartley, and M. Reid, "Subterahertz refractive flat-top beam shaping via 3D printed aspheric lens combination," *Appl. Opt.*, vol. 59, no. 18, pp. 5429–5436, 2020.

[14] O. Bouzid, A. Hasnaoui, and K. Ait-Ameur, "Simple intra-cavity beam shaping for generating a shape-invariant flat-top laser beam," *Optik*, vol. 201, 2020, Art. no. 163494.

[15] M. H. Zhang, X. L. Liu, L. N. Guo, L. Liu, and Y. J. Cai, "Partially coherent flat-topped beam generated by an Axicon," *Appl. Sci.*, vol. 9, no. 7, 2019, Art. no. 1499.

[16] A. N. K. Reddy and V. Pal, "Robust design of diffractive optical elements for forming flat-top beams with extended depth of focus," *Appl. Phys. B*, vol. 125, no. 12, 2019, Art. no. 231.

[17] H. B. Zhu, X. H. Fu, S. L. Fan, L. Liang, X. C. Lin, and Y. Q. Ning, "The conversion from a Gaussian-like beam to a flat-top beam in the laser hardening processing using a fiber coupled diode laser source," *Opt. Laser Technol.*, vol. 125, 2020, Art. no. 106028.

[18] P. F. Liu, J. Yan, W. Li, and Y. K. Wu, "Transverse mode analysis for free-space laser beams using Bayesian analysis," *Appl. Opt.*, vol. 60, no. 12, pp. 3344–3352, 2021.

[19] Y. An et al., "Fast modal analysis for Hermite–Gaussian beams via deep learning," *Appl. Opt.*, vol. 59, no. 7, pp. 1954–1959, 2020.

[20] M. Santarsiero, F. Gori, R. Borghi, and G. Guattari, "Evaluation of the modal structure of light beams composed of incoherent mixtures of Hermite-Gaussian modes," *Appl. Opt.*, vol. 38, no. 25, pp. 5272–5281, 1999.

[21] S. Volotovskiy and D. Savelyev, "Algorithm for approximating a beam with a given intensity by Hermite-Gaussian modes," in *Proc. IEEE Int. Conf. Inf. Technol. Nanotechnol.*, 2020, pp. 1–6.

[22] D. A. Kliner et al., "Advanced metal processing enabled by fiber lasers with tunable beam properties," *Proc. SPIE*, vol. 11981, pp. 72–85, 2022.

[23] A. Nissenbaum, N. Armon, and E. Shekel, "Dynamic beam lasers based on coherent beam combining," *Proc. SPIE*, vol. 11981, pp. 65–71, 2022.

[24] S. L. Oscurato, F. Reda, M. Salvatore, F. Borbone, P. Maddalena, and A. Ambrosio, "Shapeshifting diffractive optical devices," *Laser Photon. Rev.*, vol. 16, 2022, Art. no. 2100514.

[25] R. W. Gerchgerg and W. O. Saxton, "A practical algorithm for the determination of phase form image and diffraction plane pictures," *Optik*, vol. 35, pp. 237–246, 1972.

[26] J. S. Liu and M. R. Taghizadeh, "Iterative algorithm for the design of diffractive phase elements for laser beam shaping," *Opt. Lett.*, vol. 27, no. 16, pp. 1463–1465, 2002.

[27] W. Qu, H. Gu, Q. Tan, and G. Jin, "Precise design of two-dimensional diffractive optical elements for beam shaping," *Appl. Opt.*, vol. 54, no. 21, pp. 6521–6525, 2015.

[28] L. Huang et al., "Three-dimensional optical holography using a plasmonic metasurface," *Nature Commun.*, vol. 4, 2013, Art. no. 2808.

[29] H. Wang, W. Yue, Q. Song, J. Liu, and G. Situ, "A hybrid Gerchberg-Saxton-like algorithm for DOE and CGH calculation," *Opt. Laser Eng.*, vol. 89, pp. 109–115, 2017.

[30] C. Wu, J. Ko, R. Rzasa, D. A. Paulson, and C. C. Davis, "Phase and amplitude beam shaping with two deformable mirrors implementing input plane and Fourier plane phase modifications," *Appl. Opt.*, vol. 57, no. 9, pp. 2337–2345, 2018.

[31] I. M. Vellekoop and A. P. Mosk, "Focusing coherent light through opaque strongly scattering media," *Opt. Lett.*, vol. 32, no. 16, pp. 2309–2311, 2007.

[32] Z. Chen, X. Hu, X. Ji, and J. Pu, "Needle beam generated by a laser beam passing through a scattering medium," *IEEE Photon. J.*, vol. 10, no. 5, Oct. 2018, Art. no. 6501108.

[33] H. li, Z. Yu, T. Zhong, and P. Lai, "Performance enhancement in wavefront shaping of multiply scattered light: A review," *J. Biomed. Opt.*, vol. 29, 2024, Art. no. S11512.

[34] H. Li et al., "Generation of controllable spectrum in multiple positions from speckle patterns," *Opt. Laser Tech.*, vol. 149, 2022, Art. no. 107820.

[35] Y. F. Chen, C. C. Lee, C. H. Wang, and M. X. Hsieh, "Laser transverse modes of spherical resonators: A review," *Chin. Opt. Lett.*, vol. 18, 2020, Art. no. 091404.

[36] W. Kong, A. Sugita, and T. Taira, "Generation of Hermite–Gaussian modes and vortex arrays based on two-dimensional gain distribution controlled microchip laser," *Opt. Lett.*, vol. 37, pp. 2661–2663, 2012.

[37] S. Chu, Y. Chen, K. Tsai, and K. Otsuka, "Generation of high-order Hermite-Gaussian modes in end-pumped solid-state lasers for square vortex array laser beam generation," *Opt. Exp.*, vol. 20, pp. 7128–7141, 2012.

[38] Y. F. Chen, T. M. Huang, K. H. Lin, C. F. Kao, C. L. Wang, and S. C. Wang, "Analysis of the effect of pump position on transverse modes in fiber-coupled laser-diode end pumped lasers," *Opt. Commun.*, vol. 136, pp. 399–404, 1997.

[39] A. E. Siegman, *Lasers*. Melville, NY, USA: Univ. Sci. Books, 1986.

[40] D. B. Conkey, A. N. Brown, A. M. Caravaca-Aguirre, and R. Piestun, "Genetic algorithm optimization for focusing through turbid media in noisy environments," *Opt. Exp.*, vol. 20, no. 5, pp. 4840–4849, 2012.

[41] H. X. He, Y. F. Guan, and J. Y. Zhou, "Image restoration through thin turbid layers by correlation with a known object," *Opt. Exp.*, vol. 21, no. 10, pp. 12539–12545, 2013.